

## Thermally Driven Out-of-Equilibrium Two-Impurity Kondo System

Miguel A. Sierra,<sup>1</sup> Rosa López,<sup>1</sup> and Jong Soo Lim<sup>2</sup>

<sup>1</sup>*Institut de Física Interdisciplinària i de Sistemes Complexos IFISC (CSIC-UIB), E-07122 Palma de Mallorca, Spain*

<sup>2</sup>*School of Physics, Korea Institute for Advanced Study, Seoul 130-722, Korea*



(Received 13 February 2018; published 29 August 2018)

The archetypal two-impurity Kondo problem in a serially coupled double quantum dot is investigated in the presence of a thermal bias  $\theta$ . The slave-boson formulation is employed to obtain the nonlinear thermal and thermoelectrical responses. When the Kondo correlations prevail over the antiferromagnetic coupling  $J$  between dot spins, we demonstrate that the setup shows negative differential thermal conductance regions behaving as a thermal diode. In addition, we report a sign reversal of the thermoelectric current  $I(\theta)$  controlled by  $t/\Gamma$  ( $t$  and  $\Gamma$  denote the interdot tunnel and reservoir-dot tunnel couplings, respectively) and  $\theta$ . All these features are attributed to the fact that at large  $\theta$  both  $Q(\theta)$  (heat current) and  $I(\theta)$  are suppressed regardless of the value of  $t/\Gamma$  because the double dot decouples at high thermal biases. Finally, for a finite  $J$ , we investigate how the Kondo-to-antiferromagnetic crossover is altered by  $\theta$ .

DOI: 10.1103/PhysRevLett.121.096801

**Introduction.**—The richness of the single-impurity Anderson model has been nicely exhibited in singly occupied quantum dots (QDs) attached to electronic reservoirs, in which the Kondo effect is its most prominent feature [1–3]. Such artificial systems allow us an unprecedented benefit to investigate out-of-equilibrium many-body effects with the additional intriguing possibility of tuning the parameters controlling its physics [4–7]. The Kondo effect is built from the antiferromagnetic (AFM) correlations between the delocalized electrons at the reservoirs and the localized spin in the QD [8]. It is reflected in the differential conductance as a peak of height  $2e^2/h$  [9] and width  $\approx k_B T_K$  at zero applied voltage called the zero bias anomaly ( $k_B = 1$  is the Boltzmann constant and  $T_K$  corresponds to the Kondo temperature). Importantly, the recent experimental boost on quantum transport through correlated quantum systems has opened a new arena: the out-of-equilibrium Kondo physics in more intricate nanostructures such as artificial coupled Kondo systems [10–15]. The paradigmatic two-impurity Kondo system (2IKS) [16–22] possesses a quantum phase transition (QPT) in which the critical point is a two-channel Kondo fixed point [23–26] recently observed in QDs [27,28]. Such a QPT is, indeed, a consequence of the competition between the Kondo effect and the spin-to-spin interaction, the latter attributed to the Ruderman-Kittel-Kasuya-Yosida interaction [29,30], which couples two localized spins through its interaction with the delocalized electrons. Therefore, for an antiferromagnetic exchange coupling  $J > 0$  the spins exist in a singlet state [31–34]. In a Kondo dominant regime  $T_K \gg J$ , each localized spin exhibits a Kondo singularity, whereas for  $J \gg T_K$  the spins are locked into a singlet state with suppressed Kondo correlations. In the context of artificial Kondo molecules,

the antiferromagnetic interaction is generated via a superexchange mechanism with  $J \approx 4t^2/U$ , with  $t$  the interdot tunneling coupling and  $U$  the interdot Coulomb repulsion strength. Now, the connection between both reservoirs transforms the QPT into a crossover [31–33,35–39]. Different theoretical techniques, like numerical renormalization group [34,40–42] and others [32,33,43], have been applied to a deeper understanding of the 2IKS; most of them are applicable at equilibrium and only a few are focused on the nonequilibrium configuration [29,35,37–39,44,45]. Experimentally, the behavior of the 2IKS has been probed in tunnel-coupled QDs [10–15].

However, out-of-equilibrium physics in the 2IKS has been analyzed only with electric fields. A much less investigated situation is when a thermal gradient  $\theta = T_L - T_R$  [ $T_L$  ( $T_R$ ) is the temperature of the left (right) reservoir] is applied. Strong thermoelectrical response has been demonstrated to occur in confined nanostructures such as QDs [46–51]. These systems allow us to partially convert electricity into heat, and vice versa, with large Seebeck coefficients [52]. In particular, the case of a thermally biased QD in the Kondo regime has been investigated recently, mostly in the linear regime [53]. In Ref. [54] it was shown that Kondo correlations are destroyed with  $\theta$ , but more slowly than with the applied voltage  $V_{sd}$ . Additionally, it was found that the thermoelectric current  $I(\theta)$  exhibits a nontrivial zero in the Kondo regime at a critical thermal bias  $\theta_c \approx T_K$ . Consequently, the sign of  $I(\theta)$  can be controlled externally by varying  $\theta$ . A sign reversal of  $I(\theta)$  is a very unusual phenomenon that has been recently reported to happen in single quantum dots in the Coulomb blockade regime [55] and in tubular nanowires in the presence of a magnetic field as its sign control parameter [56].

In this work, we focus on the nonlinear response of a thermally biased 2IKS (see Fig. 1). Remarkably, with  $T_K \gg J$ , we find that a thermal bias perturbs our serial double quantum dot (DQD) differently depending on the ratio between the dot-lead ( $\Gamma$ ) and interdot tunneling ( $t$ ) couplings. We report situations where the DQD setup operates as a thermal diode [57] exhibiting a region of negative differential thermal conductance for sufficiently large temperature biases. Thermal diodes are of great importance for their potential applications as coolers [58], energy harvesters [59], or thermal memory storage [60], and in the emergent field of coherent caloritronics [61].

In contrast, when  $J > T_K$ , the dependence of  $T_K$  for each dot on  $\theta$  has a strong impact on the Kondo-to-antiferromagnetic crossover.

*Model Hamiltonian and theoretical approach.*—Our system illustrated in Fig. 1 consists of a tunnel-coupled DQD where each dot is connected to an electronic reservoir acting as an artificial Kondo molecule. The Hamiltonian describing this system reads

$$\mathcal{H} = \mathcal{H}_C + \mathcal{H}_D + \mathcal{H}_T. \quad (1)$$

$\mathcal{H}_C = \sum_{\alpha,k,\sigma} \varepsilon_{ak} c_{ak\sigma}^\dagger c_{ak\sigma}$  describes the fermionic reservoirs.  $c_{ak\sigma}^\dagger$  ( $c_{ak\sigma}$ ) creates (annihilates) an electron of energy  $\varepsilon_{ak}$  with wave number  $k$  and spin  $\sigma = \{\uparrow, \downarrow\}$  in the reservoir  $\alpha = \{L, R\}$ . The dot Hamiltonian is expressed in the form  $\mathcal{H}_D = \sum_{\alpha,\sigma} \varepsilon_\alpha d_{\alpha\sigma}^\dagger d_{\alpha\sigma} + U n_{\alpha\uparrow} n_{\alpha\downarrow} + \sum_{\sigma} t d_{L\sigma}^\dagger d_{R\sigma} + \text{H.c.}$  ( $d_{\alpha\sigma}^\dagger$  ( $d_{\alpha\sigma}$ ) creates (annihilates) an electron of energy  $\varepsilon_\alpha$  with spin  $\sigma$  in the dot  $\alpha$  and  $n_{\alpha\sigma} = d_{\alpha\sigma}^\dagger d_{\alpha\sigma}$  denotes the dot occupation operator. Electrons hop between dots with a tunnel amplitude  $t$ . Two electrons located in the same dot feel the on-site Coulomb interaction  $U$ .  $\mathcal{H}_T = \sum_{\alpha k \sigma} V_\alpha c_{\alpha k \sigma}^\dagger d_{\alpha \sigma} + \text{H.c.}$  connects each dot to its respective reservoir with tunneling amplitude  $V_\alpha$ .

To observe thermal and thermoelectric effects, we raise the temperature of the left reservoir by an amount of  $\theta > 0$  with respect to the background temperature such that  $T_L = T_b + \theta$  and  $T_R = T_b$ . With this configuration, our analysis proceeds in two directions: (i) the Kondo dominant case with a negligible  $J \approx 0$  and (ii) the crossover from Kondo-to-AFM phases for  $J \neq 0$ .

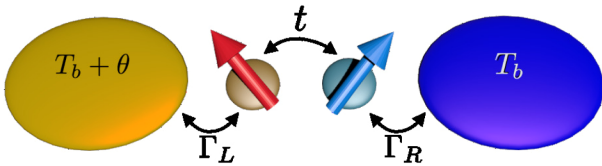


FIG. 1. Schematic of a tunnel-coupled DQD system. Each reservoir is coupled to its respective dot with the tunnel hybridization  $\Gamma_{L/R}$  and the dots are coupled with a tunnel amplitude  $t$ . The left reservoir is heated; meanwhile, the right reservoir remains at the background temperature  $T_b$  giving rise to a temperature gradient  $\theta$  in the system.

We consider the infinite- $U$  limit, thereby each dot is singly occupied for  $\varepsilon_\alpha < 0$ . Then, at very low temperatures, we can adopt a Fermi liquid description [62]. In such a case the Hamiltonian is reformulated employing the slave-boson representation. The dot operators become  $d_{\alpha\sigma}^\dagger = f_{\alpha\sigma}^\dagger b_\alpha$ . The bosonic operator  $b_\alpha$  annihilates an empty state, while the auxiliary fermion operator  $f_{\alpha\sigma}^\dagger$  creates the singly occupied state with spin  $\sigma$  at the dot  $\alpha$ . The single occupancy constraint  $b_\alpha^\dagger b_\alpha + \sum_{\sigma} f_{\alpha\sigma}^\dagger f_{\alpha\sigma} = 1$  is enforced by introducing Lagrange multipliers  $\Lambda_\alpha$ . We apply a  $1/N$  expansion, with  $N$  as the level degeneration of the dot angular momentum, here  $N = 2$ , and keep the leading order. Then, the bosonic operators are replaced by their mean-field (MF) values  $\langle b_\alpha \rangle \rightarrow \sqrt{N} \tilde{b}_\alpha$ , neglecting the fluctuations around its expectation value. The MF approach has been successfully applied to a number of Kondo-related problems [21,31,33,62], such as double-dot systems driven out of equilibrium [29,38,44,45]. We obtain a set of MF equations, i.e., the boson equation of motion and the Lagrange condition. By solving these equations, we determine the Kondo impurity parameters ( $\Lambda_\alpha, \tilde{b}_\alpha$ ) that renormalize the system parameters as  $\tilde{\varepsilon}_\alpha = \varepsilon_\alpha + \Lambda_\alpha$  and  $\tilde{\Gamma}_\alpha = \Gamma_\alpha |\tilde{b}_\alpha|^2$  with  $\Gamma_\alpha = \pi \rho_\alpha |V_\alpha|^2$  and  $\rho_\alpha$  as the density of states of the reservoir  $\alpha$  considered constant in a bandwidth  $D$ . Additionally,  $\tilde{\Gamma}_{L/R}$  and  $\tilde{\varepsilon}_{L/R}$  represent the effective Kondo temperatures  $T_{KL/R}$  and the Kondo resonance positions within this approach. The details of the calculation of  $\tilde{\varepsilon}_\alpha$  and  $\tilde{\Gamma}_\alpha$  can be found in the Supplemental Material [63].

The electric and heat current flowing out of the left reservoir ( $I = I_L$  and  $Q = Q_L$ ) are obtained by applying the commutator with  $\mathcal{H}$ , giving the result

$$I = \frac{e}{h} \int d\omega [f_L(\omega) - f_R(\omega)] \mathcal{T}(\omega), \quad (2)$$

$$Q = \frac{1}{h} \int d\omega [f_L(\omega) - f_R(\omega)] (\omega - \mu_\alpha) \mathcal{T}(\omega), \quad (3)$$

where  $e > 0$ . The Fermi-Dirac distribution of the reservoir  $\alpha$  with the chemical potential  $\mu_\alpha$  is denoted as  $f_\alpha(\omega) = 1 / \{1 + \exp[(\omega - \mu_\alpha) / k_B T_\alpha]\}$ . The analytical expressions for the transmission  $\mathcal{T}(\omega)$  and derivations for charge and heat flows are given in the Supplemental Material [63]. We emphasize that such currents have a nontrivial dependence on  $\theta$  through the MF parameters.

*Results (I): Thermally driven Kondo regime.*—At this stage we focus on a negligible  $J \approx 0$  value. Hereafter, we consider a symmetric double-dot system:  $\varepsilon_0 \equiv \varepsilon_L = \varepsilon_R = -3.5\Gamma$  and  $\Gamma_L = \Gamma_R = \Gamma$ . We set  $D = 100\Gamma$  with a background temperature  $T_b = 10^{-5}\Gamma$ , thereby,  $T_b \ll T_{K0}$ , where  $T_{K0} = D \exp[\pi\varepsilon_0/\Gamma]$  denotes the Kondo temperature for a single dot [8], where  $T_{K0} = 0.0016\Gamma$  for the chosen bare system parameters. For a serial DQD, the characteristic

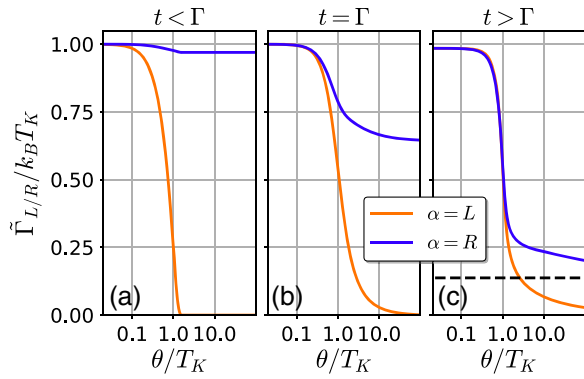


FIG. 2.  $\tilde{\Gamma}_{L/R}$  as a function of the thermal bias  $\theta$ . The left, middle, and right columns correspond to the weak ( $t = 0.25\Gamma$ ), intermediate ( $t = \Gamma$ ), and the strong coupling regimes ( $t = 2.5\Gamma$ ), respectively. The parameters are normalized by the common Kondo temperature  $T_K$  (for the definition of  $T_K$ , see the main text). Parameters are  $k_B = 1$ ,  $\Gamma_L = \Gamma_R = \Gamma$ ,  $\varepsilon_L = \varepsilon_R = -3.5\Gamma$ ,  $T_b = 10^{-5}\Gamma$ ,  $D = 100\Gamma$ ,  $\mu_{L,R} = \varepsilon_F = 0$ .

Kondo temperature is normalized by the tunneling amplitude accordingly to  $T_K = T_{K0} \exp[(t/\Gamma) \tan^{-1}(t/\Gamma)] / \sqrt{1 + (t/\Gamma)^2}$  [33]. First, we explore in Fig. 2 the behavior of the MF parameters  $\tilde{\Gamma}_\alpha$  and  $\tilde{\varepsilon}_\alpha$  when a thermal gradient  $\theta$  is applied. We distinguish three different scenarios, namely, (i) the weakly coupling regime  $t/\Gamma < 1$ , (ii) the intermediate  $t/\Gamma \sim 1$ , and (iii) the strong coupling regime  $t/\Gamma > 1$ . Then, when  $t/\Gamma < 1$  [see Fig. 2(a)] we observe that  $\tilde{\Gamma}_L(\theta)$  and  $\tilde{\Gamma}_R(\theta)$  behave very differently with  $\theta$ . Here,  $\tilde{\Gamma}_L$  (hot reservoir) decreases rapidly as  $\theta$  increases, whereas  $\tilde{\Gamma}_R$  remains almost unaffected by  $\theta$ . Each dot develops an independent Kondo resonance with its own reservoir that yields a much lower Kondo temperature for the hot reservoir that decreases its value as long as  $\theta$  augments. However, when  $t/\Gamma \approx 1$ , both  $\tilde{\Gamma}_L$  and  $\tilde{\Gamma}_R$  are affected as shown in Fig. 2(b) due to the moderate coupling between the Kondo resonances. Eventually, for  $t/\Gamma > 1$ , the DQD behaves effectively as a Kondo coherent molecule exhibiting bonding and antibonding Kondo states. Here,  $\tilde{\Gamma}_L$  and  $\tilde{\Gamma}_R$  are similar when  $\theta$  is tuned. However, at large  $\theta$ , Kondo correlations disappear in the hotter side. In such a case, the right dot decouples completely from the left dot and  $\tilde{\Gamma}_R$  approaches  $T_{K0}$ , as indicated by the dashed line in Fig. 2(c). Consequently, for very large  $\theta$  values the transport through the double dot is blocked even though Kondo correlations in the right (cold) dot take place.

All previous features determine the characteristic behaviors of the heat  $Q(\theta)$  and thermoelectric current  $I(\theta)$ . Figure 3(a) displays  $Q(\theta)$  for different interdot tunnel couplings indicating the regimes (i)  $t = 0.25\Gamma$ , (ii)  $t = \Gamma$ , and (iii)  $t = 1.5\Gamma$ ,  $2.5\Gamma$ .  $Q(\theta)$  is always positive as expected. We observe that  $Q(\theta)$  presents a maximum at a certain critical  $\theta_c$ . Then, a region of diminishing heat current appears for  $\theta > \theta_c$  exhibiting a negative differential

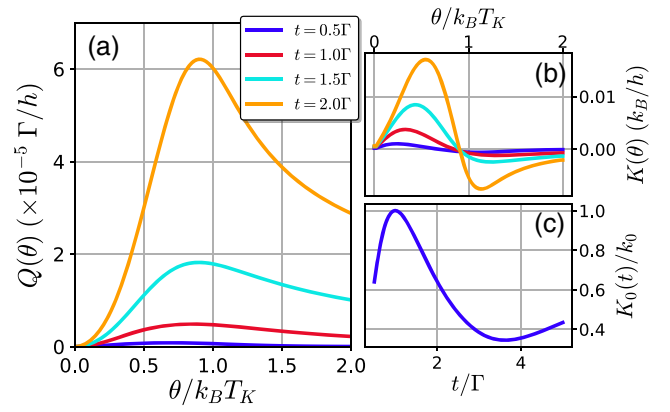


FIG. 3. (a) Heat current  $Q(\theta)$  for different values of the tunnel coupling  $t$ . (b) Differential thermal conductance  $K(\theta) = dQ/d\theta$  for different values of the tunnel coupling  $t$ . (c) Linear thermal conductance  $K_0(t)$  normalized with the thermal conductance quantum  $k_0$  as a function of the tunnel amplitude  $t$ . This result is equivalent to the transmission function at the Fermi level,  $K_0(t) = k_0 \mathcal{T}(\omega = 0, t)$ . Same parameters as in Fig. 2.

thermal conductance: the basis of a thermal diode. Here, the DQD system allows the heat flow to occur in one direction preferentially [57].

In the linear regime ( $\theta \rightarrow 0$ ) the heat flow increases linearly with  $\theta$  according to the Fourier law:  $Q \approx K_0 \theta$ , with  $K_0$  the linear thermal conductance which, at low temperatures, follows  $K_0 \approx k_0 \mathcal{T}(\varepsilon_F)$ , where  $k_0$  is the thermal conductance quantum [see Fig. 3(c)], whereas for  $\theta \rightarrow \infty$  the heat flow is suppressed since Kondo correlations at the hot reservoir are efficiently suppressed. More explicitly, this result is observed in the nonlinear thermal conductance  $K(\theta) = dQ/d\theta$  in Fig. 3(b), where by increasing  $\theta$  it makes  $K(\theta)$  change sign indicating that the DQD setup decouples due to a much smaller renormalized tunneling amplitude  $\tilde{t} = t \tilde{b}_L \tilde{b}_R$ . As a consequence, we claim that the Wiedemann-Franz law is fulfilled as long as the system behaves as a Fermi liquid ( $\theta < T_K$ ).

The thermoelectric transport of the system is characterized by the thermocurrent  $I(\theta)$  depicted in Fig. 4(a). In contrast to the heat current,  $I(\theta)$  shows distinctive differences depending on  $t/\Gamma$ . For  $t/\Gamma < 1$ ,  $I(\theta)$  is always positive, the transmission has a single peak centered at the positive frequency side; i.e., the thermocurrent has an electron-dominant character [see Fig. 4(b)] [54,55]. Increasing  $\theta$  makes the peak of  $\mathcal{T}(\omega)$  narrower, and eventually at larger  $\theta$  such shrinking yields a suppressed  $I(\theta)$ . When  $t/\Gamma > 1$ , the transmission exhibits a double peak structure due to the formation of coherent bonding and antibonding states. The transition from a single-peak transmission when  $t/\Gamma < 1$  to a double-peak transmission for  $t/\Gamma > 1$  induces a sign change in  $I(\theta)$  for some range of  $\theta$  values [see Fig. 4(c)]. The explanation for such sign reversal in  $I(\theta)$  is shown in Fig. 4(c), where the double-dot transmission is plotted for  $t = 1.5\Gamma$  at a small  $\theta$  value.

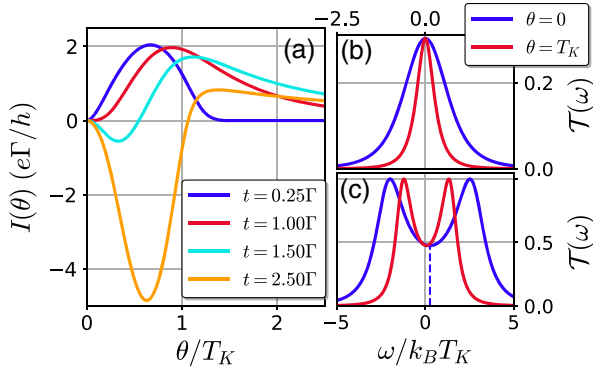


FIG. 4. (a) Thermoelectric current  $I(\theta)$  for different values of the interdot tunnel coupling  $t$ . For clarity, all curves are rescaled with the factors:  $10^{-6}$ ,  $10^{-5}$ ,  $5 \times 10^{-5}$ , and  $10^{-4}$  for  $t = 0.25\Gamma$ ,  $\Gamma$ ,  $1.5\Gamma$ , and  $t = 2.5\Gamma$ , respectively. Panels (b) and (c) show transmission probabilities  $\mathcal{T}(\omega)$  for  $t/\Gamma < 1$  and  $t/\Gamma > 1$ , respectively. Two different  $\theta$  values are considered. The dashed line in (c) indicates the position of local minimum showing that the transmission is not symmetric. Same parameters as in Fig. 2.

Notice that the transmission has more weight located at the negative frequency side in  $\mathcal{T}(\omega)$  causing a holelike flow which gives negative  $I(\theta)$ . By increasing  $\theta \approx T_K$ , the weight on the positive frequency side in  $\mathcal{T}(\omega)$  starts to contribute, adding an electronlike flow to  $I(\theta)$ . Therefore, there is a temperature  $\theta^*$  where the hole and electron contributions to  $I(\theta)$  compensate each other, yielding a vanishing thermoelectric current. Eventually, when  $\theta > \theta^*$ , the weights on positive frequencies in  $\mathcal{T}(\omega)$  dominate and therefore  $I(\theta) > 0$ . Eventually at large  $\theta$ ,  $I(\theta)$  vanishes again since Kondo correlations on the hot dot are fully suppressed and hence left and right reservoirs become uncoupled.

*Results (II): Thermally driven Kondo-to-antiferromagnetic crossover.*—In contrast to the results explained above, when  $T_K$  becomes smaller, the presence of  $J$  is unavoidable, inducing the Kondo-to-AFM transition. Therefore, we now include a non-negligible AFM interaction  $J > 0$  between localized spins  $S_{L/R}$  by adding the following term to the general Hamiltonian  $\mathcal{H}_J = 1/4JS_L \cdot S_R$  [31].

When  $J$  exceeds a critical value  $J_c$ , the localized dot spins favor the formation of an AFM spin singlet state that blocks the charge transport. In serially coupled dots, several works have reported a crossover from the Kondo regime towards an AFM single state between the dot spins [11,14,15]. Such an AFM singlet state is manifested in the nonlinear conductance  $\mathcal{G}$  exhibiting a splitting of value  $\delta \approx 2J$  [29,33,45]. Additionally, the critical value  $J_c$  has been demonstrated to take the value [29]

$$J_c/T_{KR} \approx \frac{4}{\pi} \left( 1 + \frac{T_{KL}}{T_{KR}} \right), \quad (4)$$

where  $T_{KR} > T_{KL}$ . Previously, we showed that a thermal bias alters dramatically the behavior of the Kondo scales

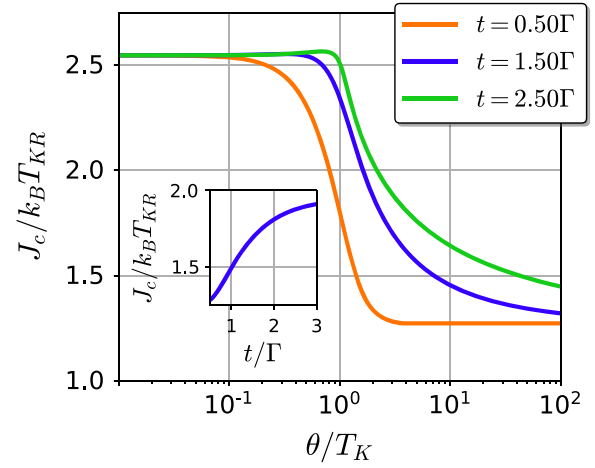


FIG. 5.  $J_c/k_B T_{KR}$  for several values of the interdot tunnel coupling  $t/\Gamma$ . Inset:  $J_c/k_B T_{KR}$  as a function of  $t/\Gamma$  at  $\theta = 3.1T_K$ . Same parameters as in Fig. 2.

$T_{KL} (\approx \tilde{\Gamma}_L)$  and  $T_{KR} (\approx \tilde{\Gamma}_R)$ . Therefore, according to Eq. (4),  $\theta$  affects the value of  $J_c$ . In Fig. 5, we depict  $J_c/T_{KR}$  when  $\theta$  is tuned for different  $t/\Gamma$ . The overall tendency is a transition from  $J_c/T_{KR} \approx 8/\pi$  towards  $J_c/T_{KR} \approx 4/\pi$  at large  $\theta$  due to the suppression of the Kondo correlations in the hot dot  $T_{KL} \approx 0$ . The inset of Fig. 5 displays the behavior of the critical value  $J_c/T_{KR}$  for a fixed  $\theta = 3.25T_K$  as a function of  $t/\Gamma$ .  $J_c/T_{KR}$  increases with  $t/\Gamma$  because Kondo correlations (for low or moderate  $\theta$  values) are reinforced when the interdot tunneling coupling  $t/\Gamma$  increases. Consequently, a stronger AFM coupling is needed to suppress Kondo correlations.

*Summary.*—Summarizing, the two-impurity Kondo system driven by a thermal bias  $\theta$  has been examined. When Kondo correlations are dominant ( $J = 0$ ),  $\theta$  has a strong influence on the Kondo scales and consequently on the transport properties of the Kondo-based setups. Our findings indicate that for sufficiently large  $\theta$  the Kondo correlations are destroyed for the dot coupled to the hot reservoir regardless of the interdot strength coupling. Since the interdot coupling is renormalized by the Kondo correlations for both dots, the DQD setup gets decoupled leading to suppressed electrical and heat flows. For non-negligible antiferromagnetic spin exchange coupling, we report the influence of  $\theta$  on the Kondo-to-AFM crossover. For a finite  $J$ , we find that such a crossover takes place around a critical value that for a small  $\theta$  takes the value  $J_c/T_{KR} = 8/\pi$ , whereas for a large  $\theta$ ,  $J_c$  reaches the value of  $\approx 4/\pi$ . This result is due to the quenching Kondo correlations on the hot reservoir when  $\theta$  augments. Finally, we highlight that all our observations might be experimentally tested due to the huge progress on thermoelectrical transport through nanostructures.

We are grateful to D. Sánchez for helpful discussions. This work was supported by the MINECO Grants No. FIS2014-52564 and No. MAT2017-82639 and the predoctoral grant from the government of Balearic Islands (CAIB).

- 
- [1] T. K. Ng and P. A. Lee, On-Site Coulomb Repulsion and Resonant Tunneling, *Phys. Rev. Lett.* **61**, 1768 (1988).
- [2] L. I. Glazman and M. É. Raïkh, Resonant Kondo transparency of a barrier with quasilocal impurity states, *JETP Lett.* **47**, 452 (1988).
- [3] A. Kawabata, On the electron transport through a quantum dot, *J. Phys. Soc. Jpn.* **60**, 3222 (1991).
- [4] D. Goldhaber-Gordon, H. Shtrikman, D. Mahalu, D. Abusch-Magder, U. Meirav, and M. A. Kastner, Kondo effect in a single-electron transistor, *Nature (London)* **391**, 156 (1998).
- [5] S. M. Cronenwett, T. H. Oosterkamp, and L. P. Kouwenhoven, A tunable Kondo effect in quantum dots, *Science* **281**, 540 (1998).
- [6] J. Schmid, J. Weis, K. Eberl, and K. v. Klitzing, A quantum dot in the limit of strong coupling to reservoirs, *Physica (Amsterdam)* **256B**, 182 (1998).
- [7] S. Sasaki, S. De Franceschi, J. M. Elzerman, W. G. van der Wiel, M. Eto, S. Tarucha, and L. P. Kouwenhoven, Kondo effect in an integer-spin quantum dot, *Nature (London)* **405**, 764 (2000).
- [8] See, e.g., A. C. Hewson, *The Kondo Problem to Heavy Fermions* (Cambridge University Press, Cambridge, England, 1993).
- [9] W. G. van der Wiel, S. De Franceschi, T. Fujisawa, J. M. Elzerman, S. Tarucha, and L. P. Kouwenhoven, The Kondo effect in the unitary limit, *Science* **289**, 2105 (2000).
- [10] H. Jeong, A. M. Chang, and M. R. Melloch, The Kondo effect in an artificial quantum dot molecule, *Science* **293**, 2221 (2001).
- [11] N. J. Craig, J. M. Taylor, E. A. Lester, C. M. Marcus, M. P. Hanson, and A. C. Gossard, Tunable nonlocal spin control in a coupled-quantum dot system, *Science* **304**, 565 (2004).
- [12] P. Wahl, P. Simon, L. Diekhöner, V. S. Stepanyuk, P. Bruno, M. A. Schneider, and K. Kern, Exchange Interaction between Single Magnetic Adatoms, *Phys. Rev. Lett.* **98**, 056601 (2007).
- [13] N. Néel, R. Berndt, J. Kröger, T. O. Wehling, A. I. Lichtenstein, and M. I. Katsnelson, Two-Site Kondo Effect in Atomic Chains, *Phys. Rev. Lett.* **107**, 106804 (2011).
- [14] S. J. Chorley, M. R. Galpin, F. W. Jayatilaka, C. G. Smith, D. E. Logan, and M. R. Buitelaar, Tunable Kondo Physics in a Carbon Nanotube Double Quantum Dot, *Phys. Rev. Lett.* **109**, 156804 (2012).
- [15] M. Larsson, J. S. Lim, R. López, and H. Q. Xu, Tunable zero-field Kondo splitting in a quantum dot, *Phys. Rev. B* **88**, 085407 (2013).
- [16] S. Alexander and P. W. Anderson, Interaction between localized states in metals, *Phys. Rev.* **133**, A1594 (1964).
- [17] C. Jayaprakash, H. R. Krishna-murthy, and J. W. Wilkins, Two-Impurity Kondo Problem, *Phys. Rev. Lett.* **47**, 737 (1981).
- [18] B. A. Jones and C. M. Varma, Study of Two Magnetic Impurities in a Fermi Gas, *Phys. Rev. Lett.* **58**, 843 (1987).
- [19] B. A. Jones, C. M. Varma, and J. W. Wilkins, Low-Temperature Properties of the Two-Impurity Kondo Hamiltonian, *Phys. Rev. Lett.* **61**, 125 (1988).
- [20] B. A. Jones and C. M. Varma, Critical point in the solution of the two magnetic impurity problem, *Phys. Rev. B* **40**, 324 (1989).
- [21] B. A. Jones, B. G. Kotliar, and A. J. Millis, Mean-field analysis of two antiferromagnetically coupled Anderson impurities, *Phys. Rev. B* **39**, 3415 (1989).
- [22] B. A. Jones, Pair correlation effects in heavy fermions, *Physica (Amsterdam)* **171B**, 53 (1991).
- [23] I. Affleck and A. W. W. Ludwig, Exact Critical Theory of the Two-Impurity Kondo Model, *Phys. Rev. Lett.* **68**, 1046 (1992).
- [24] J. Gan, Mapping the Critical Point of the Two-Impurity Kondo Model to a Two-Channel Problem, *Phys. Rev. Lett.* **74**, 2583 (1995).
- [25] G. Zaránd, C.-H. Chung, P. Simon, and M. Vojta, Quantum Criticality in a Double-Quantum-Dot System, *Phys. Rev. Lett.* **97**, 166802 (2006).
- [26] F. W. Jayatilaka, M. R. Galpin, and D. E. Logan, Two-channel Kondo physics in tunnel-coupled double quantum dots, *Phys. Rev. B* **84**, 115111 (2011).
- [27] R. M. Potok, I. G. Rau, H. Shtrikman, Y. Oreg, and D. Goldhaber-Gordon, Observation of the two-channel Kondo effect, *Nature (London)* **446**, 167 (2007).
- [28] A. J. Keller, L. Peeters, C. P. Moca, I. Weymann, D. Mahalu, V. Umansky, G. Zaránd, and D. Goldhaber-Gordon, Universal Fermi liquid crossover and quantum criticality in a mesoscopic system, *Nature (London)* **526**, 237 (2015).
- [29] P. Simon, R. López, and Y. Oreg, Ruderman-Kittel-Kasuya-Yosida and Magnetic-Field Interactions in Coupled Kondo Quantum Dots, *Phys. Rev. Lett.* **94**, 086602 (2005).
- [30] E. Minamitani, W. A. Diño, W. A. H. Nakanishi, and H. Kasai, Effect of antiferromagnetic RKKY interaction and magnetic field in a two-impurity Kondo system, *Phys. Rev. B* **82**, 153203 (2010).
- [31] A. Georges and Y. Meir, Electronic Correlations in Transport through Coupled Quantum Dots, *Phys. Rev. Lett.* **82**, 3508 (1999).
- [32] C. A. Büsser, E. V. Anda, A. L. Lima, M. A. Davidovich, and G. Chiappe, Transport in coupled quantum dots: Kondo effect versus antiferromagnetic correlation, *Phys. Rev. B* **62**, 9907 (2000).
- [33] T. Aono and M. Eto, Kondo effect in coupled quantum dots under magnetic fields, *Phys. Rev. B* **64**, 073307 (2001).
- [34] O. Sakai, Y. Shimizu, and T. Kasuya, Excitation spectra of two impurity Anderson model, *Solid State Commun.* **75**, 81 (1990).
- [35] R. M. Konik, Kondo Physics and Exact Solvability of Double Dots Systems, *Phys. Rev. Lett.* **99**, 076602 (2007).
- [36] P. Simon, Kondo screening cloud in a double quantum dot system, *Phys. Rev. B* **71**, 155319 (2005).
- [37] M. G. Vavilov and L. I. Glazman, Transport Spectroscopy of Kondo Quantum Dots Coupled by RKKY Interaction, *Phys. Rev. Lett.* **94**, 086805 (2005).

- [38] B. Dong and X. L. Lei, Kondo effect and antiferromagnetic correlation in transport through tunneling-coupled double quantum dots, *Phys. Rev. B* **65**, 241304(R) (2002).
- [39] I. J. Hamad, L. C. Ribeiro, G. B. Martins, and E. V. Anda, Transport properties of a two-impurity system: A theoretical approach, *Phys. Rev. B* **87**, 115102 (2013).
- [40] R. Bulla, T. A. Costi, and T. Pruschke, Numerical renormalization group method for quantum impurity systems, *Rev. Mod. Phys.* **80**, 395 (2008).
- [41] R. Žitko, Numerical renormalization group calculations of ground-state energy: Application to correlation effects in the adsorption of magnetic impurities on metal surfaces, *Phys. Rev. B* **79**, 233105 (2009).
- [42] R. Žitko and J. Bonča, Quantum phase transitions in systems of parallel quantum dots, *Phys. Rev. B* **76**, 241305 (2007).
- [43] C. Karrasch, T. Enss, and V. Meden, Functional renormalization group approach to transport through correlated quantum dots, *Phys. Rev. B* **73**, 235337 (2006).
- [44] R. Aguado and D. C. Langreth, Out-of-Equilibrium Kondo Effect in Double Quantum Dots, *Phys. Rev. Lett.* **85**, 1946 (2000).
- [45] R. López, R. Aguado, and G. Platero, Nonequilibrium Transport through Double Quantum Dots: Kondo Effect versus Antiferromagnetic Coupling, *Phys. Rev. Lett.* **89**, 136802 (2002).
- [46] L. W. Molenkamp, H. van Houten, C. W. J. Beenakker, R. Eppenga, and C. T. Foxon, Quantum Oscillations in the Transverse Voltage of a Channel in the Nonlinear Transport Regime, *Phys. Rev. Lett.* **65**, 1052 (1990).
- [47] A. S. Dzurak, C. G. Smith, C. H. W. Barnes, M. Pepper, L. Martín-Moreno, C. T. Liang, D. A. Ritchie, and G. A. C. Jones, Thermoelectric signature of the excitation spectrum of a quantum dot, *Phys. Rev. B* **55**, R10197 (1997).
- [48] S. F. Svensson, E. A. Hoffmann, N. Nakpathomkun, P. M. Wu, H. Q. Xu, H. A. Nilsson, D. Sánchez, V. Kashcheyevs, and H. Linke, Nonlinear thermovoltage and thermocurrent in quantum dots, *New J. Phys.* **15**, 105011 (2013).
- [49] X. Chen, H. Buhmann, and L. W. Molenkamp, Thermopower of the molecular state in a double quantum dot, *Phys. Rev. B* **61**, 16801 (2000).
- [50] P. Roura-Bas, L. Tosi, A. A. Aligia, and P. S. Cornaglia, Thermopower of an SU(4) Kondo resonance under an SU(2) symmetry-breaking field, *Phys. Rev. B* **86**, 165106 (2012).
- [51] H. Thierschmann, M. Henke, J. Knorr, L. Maier, C. Heyn, W. Hansen, H. Buhmann, and L. W. Molenkamp, Diffusion thermopower of a serial double quantum dot, *New J. Phys.* **15**, 123010 (2013).
- [52] *Thermoelectrics Handbook. Macro to Nano*, edited by D. M. Rowe (CRC Press, Boca Raton, FL, 2006).
- [53] Z. Zhang, Thermopower of double quantum dots: Fano effect and competition between Kondo and antiferromagnetic correlations *J. Phys. Condens. Matter* **19**, 086214 (2007).
- [54] M. A. Sierra, D. Sánchez, and R. López, Fate of the spin-1/2 Kondo effect in the presence of temperature gradients, *Phys. Rev. B* **96**, 085416 (2017).
- [55] M. A. Sierra and D. Sánchez, Strongly nonlinear thermovoltage and heat dissipation in interacting quantum dots, *Phys. Rev. B* **90**, 115313 (2014).
- [56] S. I. Erlingsson, A. Manolescu, G. A. Nemnes, J. H. Bardarson, and D. Sanchez, Reversal of Thermoelectric Current in Tubular Nanowires, *Phys. Rev. Lett.* **119**, 036804 (2017).
- [57] B. Li, L. Wang, and G. Casati, Thermal Diode: Rectification of Heat Flux, *Phys. Rev. Lett.* **93**, 184301 (2004).
- [58] F. Giazotto, T. T. Heikkilä, A. Luukanen, A. M. Savin, and J. P. Pekola, Opportunities for mesoscopes in thermometry and refrigeration: Physics and applications, *Rev. Mod. Phys.* **78**, 217 (2006).
- [59] Y. Dubi and M. Di Ventra, Heat flow and thermoelectricity in atomic and molecular junctions, *Rev. Mod. Phys.* **83**, 131 (2011).
- [60] L. Wang and B. Li, Thermal Memory: A Storage of Phononic Information, *Phys. Rev. Lett.* **101**, 267203 (2008).
- [61] M. J. Martínez-Pérez, P. Solinas, and F. Giazotto, Coherent caloritronics in Josephson-based nanocircuits, *J. Low Temp. Phys.* **175**, 813 (2014).
- [62] P. Coleman, Mixed valence as an almost broken symmetry, *Phys. Rev. B* **35**, 5072 (1987).
- [63] See Supplemental Material at <http://link.aps.org/supplemental/10.1103/PhysRevLett.121.096801> for details.